Preparation and Properties of Nanocomposites Based on Different Polarities of Nitrile–Butadiene Rubber with Clay

Yu-Rong Liang,[1,2] Wei-Liang Cao,[2] Xiao-Bin Zhang,[1] Ying-Jie Tan,[1] Shao-Jian He,[3] Li-Qun Zhang[2,3]

[1]*The Institute of Materials Engineering, Taiyuan Institute of Technology, Taiyuan 030008, People's Republic of China*
[2]*Key Lab for Nanomaterials, Ministry of Education, Beijing University of Chemical Technology, Beijing 100029, People's Republic of China*
[3]*The Key Laboratory of Beijing City on Preparation and Processing of Novel Polymer Materials, Beijing University of Chemical Technology, Beijing, People's Republic of China*

Received 30 June 2008; accepted 27 September 2008
DOI 10.1002/app.29575
Published online 25 February 2009 in Wiley InterScience (www.interscience.wiley.com).

ABSTRACT: Nanocomposites were prepared with different grades of nitrile–butadiene rubber (NBR) [with nitrile (CN) contents of 26, 35, and 42%] with organoclay (OC) by a melt-compounding process. The rubber/clay nanocomposites were examined by transmission electron microscopy (TEM) and X-ray diffraction (XRD). An increase in the polarity of NBR affected the XRD results significantly. The dispersion level of the nanofiller in the nanocomposites was determined by a function of the polarity of the rubber, the structure of the clay, and their mutual interaction. The intercalated structure and unintercalated structure coexisted in the lower polar of NBR. In addition, a relatively uniformly dispersed state corresponded to a more intercalated structure, which existed in the higher polar of NBR matrix. Furthermore, high-pressure vulcanization changed the extent of intercalation. The mechanical properties and gas barrier properties were studied for all of the compositions. As a result, an improvement in the mechanical properties was observed along with the higher polarity of NBR. This improvement was attributed to a strong interaction of hydrogen bonding between the CN of NBR and the OH of the clay. Changes in the gas barrier properties, together with changes in the polarity of the rubbers, were explained with the help of the XRD and TEM results. The higher the CN content of the rubber was, the more easily the OC approached to the nanoscale, and the higher the gas barrier properties were. J Appl Polym Sci 112: 3087–3094, 2009

Key words: nanocomposites; organoclay; rubber

INTRODUCTION

Since the last decade of the 20th century, polymer/clay nanocomposites have emerged as a new class of material and have attracted great interest from academia and industry because polymer/clay nanocomposites exhibit significantly improved performances in comparison with their microcounterparts and macrocounterparts and their pristine polymer matrices;[1–3] these improvements include increased modulus and strength, improved heat resistance, outstanding gas barrier properties, and decreased flammability. These outstanding properties suggest the potential of discovering materials with unique hybrid properties.[4–7]

In contrast to the intense interest in thermoplastic polymer/clay nanocomposites in the past decade, investigations have only very recently started on rubber/clay nanocomposites,[8] such as composites with carboxylated nitrile–butadiene rubber, isobutyl–isoprene rubber, nature rubber, styrene–butadiene rubber, ethylene–propylene–diene monomer, and silicon rubber, with different hybrid strategies, including solution intercalation,[9,10] melt compounding,[11–15] and rubber latex route.[16–20] Among these strategies, melt compounding, in which the polymer is directly intercalated into the organoclay (OC) in the molten state to prepare nanocomposites and the driving force of the intercalation is determined by physical and/or chemical interactions between the polymers and OC, may be of great practical relevance because a rubber processing facility can be used and no organic solvent is needed.

The most important consideration in the achievement of successful rubber/clay nanocomposites is the dispersion of OC particles in the rubber matrix. On the basis of different arrangements of the silicate

Correspondence to: L.-Q. Zhang (zhanglq@mail.buct.edu.cn).

Contract grant sponsor: Distinguished Youth Scientist Foundation of National Nature Science Foundation; contract grant number: 50725310.

Contract grant sponsor: National Nature Science Foundations of China; contract grant numbers: 50873095 and 50503003.

TABLE I
Recipes of the NBR Compounds

Ingredient	Content (phr)
NBR (42NBR, 35NBR, and 26NBR)	100
OC	10
Zinc oxide	5
Stearic acid	1.5
Dibenzothiazole disulfide	1.5
Sulfur	2.0

layers in the polymer matrix, two types of morphology can be achieved in nanocomposites: intercalated or exfoliated. Compared with the intercalated structure, the exfoliated structure is well recognized as the better morphology for obtaining higher performances or reducing clay loading. However, fully exfoliated rubber/clay nanocomposites are not easy to produce at all, especially with the melt-mixing method.

Until now, little study has been done on the structure–property relationships of these rubbery polymers. Also, earlier articles on elastomers have indicated that more exhaustive studies are needed to understand the mechanism of reinforcement of the systems. There are many factors affecting the morphology of rubber/clay nanocomposites prepared by melt compounding. Some previous studies have disclosed that the dispersion state of OC in the rubber matrix is influenced by the type of intercalant,[21–24] compounding condition (shear rate and temperature),[25,26] and nature of the rubber matrix.[26,27] In this study, nitrile–butadiene rubber (NBR)/clay nanocomposites were prepared by a melt-blending process. The structure of the NBR-based nanocomposites was elucidated with X-ray diffraction (XRD) and transmission electron microscopy (TEM), and the effects of polarity on the intercalation and dispersion of OC in the rubber matrix were investigated by the mixing of OC with three grades of NBR [with different nitrile (CN) contents] to produce rubber/clay nanocomposites. The mechanical properties and gas barrier properties of the prepared composites are reported here and correlated with a function of the polarity of the rubber, the structure of the clay, and their mutual interaction.

EXPERIMENTAL

Materials and formulation

Three grades of NBR (NBR220S, NBR230S, and NBR240S) with different CN contents having a Mooney viscosity of 56 at 100°C were supplied by Japan Synthetic Rubber, Inc. (Tokyo, Japan). OC intercalated by dimethyl dialkyl (C14–C18) ammonium (Nanomer I.44P) with 65% montmorillonite was supplied by Nanocor, Inc. (Chicago, IL) The rubber additives, namely, zinc oxide, stearic acid, dibenzothiazole disulfide, and sulfur, were commercial grade.

The formulation of the NBR/OC compounds (i.e., uncured composites) is described in Table I.

Preparation of the NBR/OC compounds and NBR/OC nanocomposites

NBR220S, NBR230S, and NBR240S with OC were first compounded for about 15 min with a two-roll mill; then, the additives, zinc oxide, sulfur, stearic acid, and accelerator, were gradually mixed into the compounds. The calendered NBR/OC compound sheets, 1 mm in thickness and 200 mm in width, were removed from the rotating rolls. Some of them were used for XRD and TEM examinations. The other compounds were vulcanized in a standard mold at 160°C with 15 MPa of pressure for their optimum cure times, which were determined with a disc oscillating rheometer (P355B2, Beijing Huanfeng Chemical Technology and Experimental Machine Plant, Beijing, China).

The corresponding abbreviations and related characteristic of the materials used in this study are shown in Table II.

Measurements

XRD measurements were carried out on a Rigaku RINT diffractometer (Rigaku Inc., Sendagaya, Japan) with an incident X-ray wavelength of about 1.54 Å (Cu Kα) radiation at 40 kV and 200 mA. Basal spacing between the silicate layers was observed from 0.50 to 10° (2θ) at a scanning rate of 1°/min. TEM observations were performed on an H-800 transmission electron microscope (Hitachi Co., Tokyo, Japan) with an acceleration voltage of 200 kV at room temperature. Ultrathin sections of the NBR/OC compounds and nanocomposites for TEM observation were cryogenically cut with a glass knife at a temperature of −100°C with a Leica Ultracut UCT equipped with an EMFCS cryoattachment and were collected on copper grids.

TABLE II
Corresponding Abbreviations of the Materials Used

Trademark	CN content (%)	Clay (phr)	Cured or uncured	Abbreviation
NBR220S	42	0	Uncured	42NBR
NBR220S	42	0	Cured	Pure 42NBR
NBR220S	42	10	Uncured	U-42NBR/OCNs
NBR220S	42	10	Cured	42NBR/OCNs
NBR230S	35	0	Uncured	35NBR
NBR230S	35	0	Cured	Pure 35NBR
NBR230S	35	10	Uncured	U-35NBR/OCNs
NBR230S	35	10	Cured	35NBR/OCNs
NBR240S	26	0	Uncured	26NBR
NBR240S	26	0	Cured	Pure 26NBR
NBR240S	26	10	Uncured	U-26NBR/OCNs
NBR240S	26	10	Cured	26NBR/OCNs

Measurements of the mechanical properties of all specimens were conducted at 25 ± 2°C according to relevant ISO standards (ISO 37 and ISO 7619). For tensile tests (SANS, Shenzhen, China), a CTM 4104 tensile tester was used at a crosshead rate of 500 mm/min. The permeation experiment of nitrogen was carried out with a gas permeability measuring apparatus according to ISO 2782. The pressure was maintained at 0.57 MPa on one side of the specimen sheet (ca. l mm in thickness and 8 cm in diameter) and, initially, at zero on the other one. The nitrogen permeability was calculated from the rate of transmission through the sheet at 40°C, which was determined by gas chromatography.

RESULTS AND DISCUSSION

Microstructural and morphological analyses

XRD analysis

XRD patterns supplied useful information on the gallery size of the final intercalated hybrids by the monitoring of the basal (001) *d*-spacing. Generally, intense reflections in the range $2\theta = 2$–10° indicate an ordered intercalated system with alternating polymer/silicate layers.

XRD spectrograms of the OC, NBR/OC nanocompounds (uncured nanocomposites, abbreviated as U-NBR/OCNs), and NBR/OC nanocomposites (abbreviated as NBR/OCNs) are presented in Figure 1(a,b). The diffraction peak on the XRD spectrogram of the OC was found at $2\theta = 3.9^\circ$, which corresponded to a basal spacing of 2.2 nm. When OC was directly added to three grades of NBR matrix, a new intense and sharp reflection peak appeared at a smaller angle in both the nanocompounds and nanocomposites. In the pattern of the U-NBR/OCNs, the $d_{(001)}$ reflection peak, which corresponded to a basal spacing of about 4.1 nm, was obviously intense compared to that of the OC; moreover, its high order reflection peak, which corresponded to a basal spacing of 2.0 nm ($2\theta = 4.4^\circ$, marked with an asterisk), was obvious. In the XRD pattern of the NBR/OCNs cured at high pressure, the $d_{(001)}$ reflection peak at $2\theta = 2.3^\circ$ (~ 3.8 nm) was quite strong, and a high-order reflection peak at about 4.6° (marked with an asterisk) for an interlayer spacing of 1.9 nm was observed, which were looked on as secondary diffraction peaks and related to reflections at higher orders.[28,29] These results mean that NBR molecule chains intercalated into the interlayers of the OC and formed an ordered intercalated structure. Compared with the NBR/OCNs, the U-NBR/OCN diffraction peak of the OC registered at a slightly smaller scattering angle; the intensity of the diffraction pattern significantly decreased, which indicated that the rubber molecules dispersed uniformly in the U-NBR/OCNs. Analytically speaking,

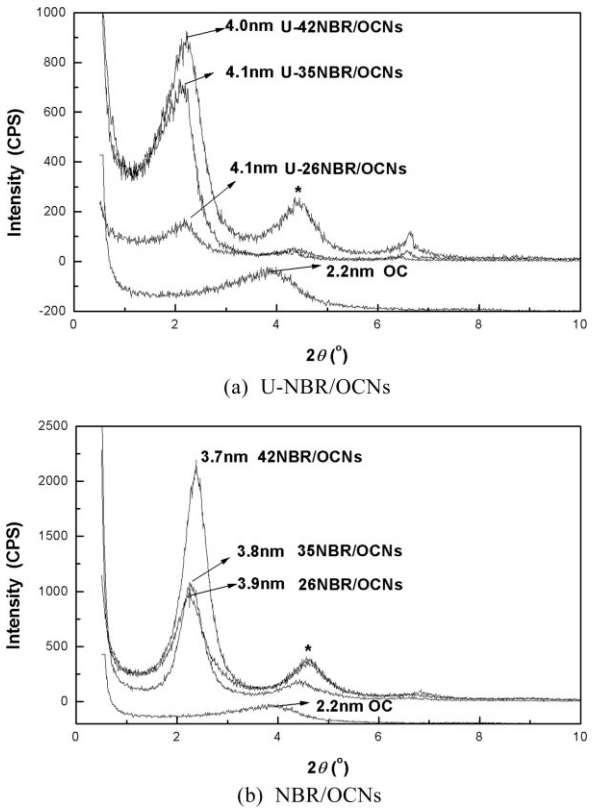

Figure 1 XRD spectrograms of OC, nanocompounds and nanocomposites: (a) U-NBR/OCNs and (b) NBR/OCNs.

the interlayer spacing of the cured nanocomposites was smaller than that of the uncured sample because of partial removal of molecular chains from the interlayer spacing of OC. Conclusively, the observed phenomena was quite the same as that in NBR/clay nanocomposites prepared by melt blending, as reported in previous article.[30] These revealed that the high-pressure vulcanization changed the extent of intercalation, which confirmed the fact that the pressure was a critical factor governing the final microstructure of the cured rubber/clay nanocomposites, as described in our earlier publication.[31]

Furthermore, an increase in the polarity of NBR (26NBR, 35NBR, and 42NBR) affected the XRD results significantly. The U-42NBR/OCNs (42NBR/OCNs) registered a peak at almost the same degree, but the intensity of the reflection peak was stronger (markedly stronger) than that of the U-35NBR/OCNs (35NBR/OCNs); similarly, the diffraction peak of the U-35NBR/OCNs (35NBR/OCNs) was considerably stronger than (nearly equal to) that of the U-26NBR/OCNs (26NBR/OCNs). This implies that the U-42NBR/OCNs (42NBR/OCNs) had a better intercalated structure than the U-35NBR/OCNs (35NBR/OCNs) in the OC gallery, and the U-35NBR/OCNs (35NBR/OCNs) had an intercalated structure that was far superior to that of the U-26NBR/OCNs (26NBR/OCNs), although none of them showed complete exfoliation.

As 26NBR had a smaller amount of CN than 35NBR and 42NBR, it may be possible that more and more polymer chains of 26NBR were needed for hydrogen bonding with the clay surface. Moreover, there would have been a nonpolar–polar interaction between the clay modifier and the polymer. Therefore, the intercalation of chains into the gallery would have been less. However, for 42NBR, a sufficient amount of CN was present. Therefore, fewer chains were sufficient to saturate the surface OHs of the OC. The remaining chains were available to intercalate into the gallery gap of the modified clay. Moreover, a greater amount of CN may have influenced the $-^{+}NH_3$ of the surface modifiers of the OC to form hydrogen bonds with CN^{-} of the polymer chains, and this may have been a facilitating factor for the 42NBR intercalation. For 35NBR, a middle amount of CN was present, so the intercalation structure was placed in the middle. As a result, there was a strong possibility of hydrogen bonding between the CN of NBR and the OH of the clay, which would have favored the intercalation of the polymer chains into the gallery gap.

In summary, the nature of the rubber controlled the extent of intercalation and the dispersion level of the nanofiller. When all of the U-NBR/OCNs (NBR/OCNs) were compared, we concluded that the higher polarity the polymers claimed, the more easily the intercalation formed.

TEM observation

Figures 2 and 3 represent the TEM images of the U-NBR/OCNs and NBR/OCNs prepared on the basis of three grades of NBR with OC, respectively.

In the case of the U-26NBR/OCNs, a portion was intercalated, whereas a number of other portions were only unintercalated silicate structures. In the case of the U-35NBR/OCNs and U-42NBR/OCNs, the OC was equally distributed within the NBR matrix, and large portions were intercalated, whereas only a small portion was nonintercalated. Compared with those in the U-26NBR/OCNs, the OC particles in the U-35NBR/OCNs and U-42NBR/OCNs were relatively more uniformly dispersed within the NBR matrix. Meanwhile, compared with those of the U-35NBR/OCNs, the dimensions of the dispersed OC were quite fine, and their spatial distributions were more homogeneous in the U-42NBR/OCNs. For example, a low-magnification TEM photograph of the U-42NBR/OCNs clearly showed that most intercalated silicate layers about 10–20 nm in width (30–50 nm for the U-35NBR/OCNs and 50–100 nm for the U-26NBR/OCNs) and 100–200 nm in length (200–300 nm for the U-35NBR/OCNs and 200–500 nm for the U-26NBR/OCNs) were homogeneously dispersed in the NBR matrix. Moreover, the intercalated silicate layers were locally stacked in some regions of the polymer matrix. A high-magnification TEM photograph also showed that there were some finer silicate particles dispersed in the NBR matrix, the width of which was within the range 4–7 nm, whereas in the U-26NBR/OCNs, the dispersion of these clay agglomerates was inhomogeneous. The enlarging observation revealed that the agglomerates were composed of many silicate tactoids. A similar conclusion could be drawn for the NBR/OCNs.

As a result, we deemed that the polar nature of the rubber was determined by amount of CN content, which was effective on the greatly improved dispersion homogeneity of the silicate layers in the U-NBR/OCNs and NBR/OCNs.

Although the dispersion of OC particles was relatively fine and their dispersion state was homogeneous in the U-NBR/OCNs, after the NBR/OC nanocompounds were cured at high pressure, the dispersion of OC particles became larger, and the dispersion homogeneity of them was reduced. These results also suggest that the initially finely dispersed OC particles could aggregate (particles comprised of orderly stacked silicate layers) to form a larger dispersion during high-pressure vulcanization. To probe further, this change in the dispersion state was more obvious in 26NBR/OC, weak in 35NBR/OC, and indistinctive in the 42NBR/OC system. There was a possibility of hydrogen-bond formation between the ammonium ion of the intercalated amine and the CN group of NBR; the strong matrix–filler interaction by hydrogen bonding in this NBR/OC compound may have overcome the curing pressure and caused the aggregation of fine OC particles. As a result, the more polarity the NBR had, the easier it was to favor fine dispersion.

This observation is in line with the XRD results, both of which indicate that the NBR/OCNs, prepared by three grades of NBR, had an ordered intercalated structure. The higher the CN content of the rubber was, the more easily the OC amounted to the nanoscale, whereas pressure had a great impact on the morphology of the rubber/clay nanocomposites.

Mechanical properties of the NBR/OCNs

The efficiency of OC in improving the mechanical properties of polymer materials is primarily determined by the degree of its dispersion in the polymer matrix.

The variation in the degree of intercalation of OC in the vulcanized NBR should manifest itself in the mechanical performances of the rubber nanocomposites. The mechanical properties of the pure NBR and NBR/OCNs are shown in Table III.

A remarkable increase in the mechanical properties, including the hardness, stresses at 100 and 300%, tensile strength, elongation at break,

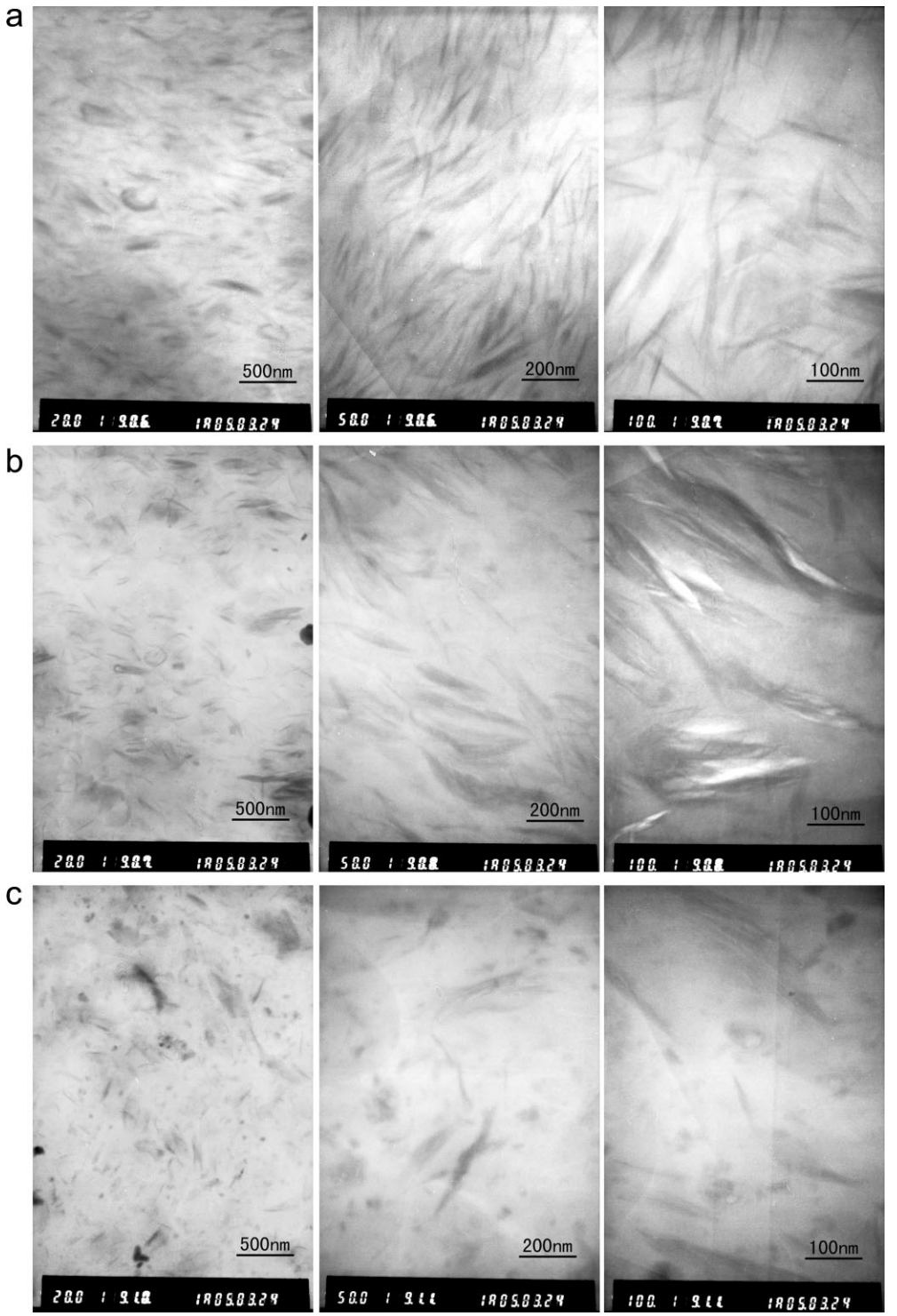

Figure 2 TEM images of NBR/OC (10 phr) nanocompounds: (a) U-42NBR/OCNs, (b) U-35NBR/OCNs, and (c) U-26NBR/OCNs.

permanent set, and tear strength, was observed for the NBR/OCNs. These qualities were all improved compared over those in the corresponding pure NBR. All these improvements could be assigned to the high aspect ratio and the nanometer dispersion of organic clay layers, which acted as an intensifier in the rubber matrix.

Generally, the strength was higher with a higher CN content of the rubber because of the higher polarity and higher glass-transition temperature[32] (T_g of 42NBR = −20°C, T_g of 35NBR = −30°C, and T_g of 26NBR = −40°C). There were 397, 332, and 85% improvements in the tensile strength of the nanocomposites prepared by modified clay with 42NBR,

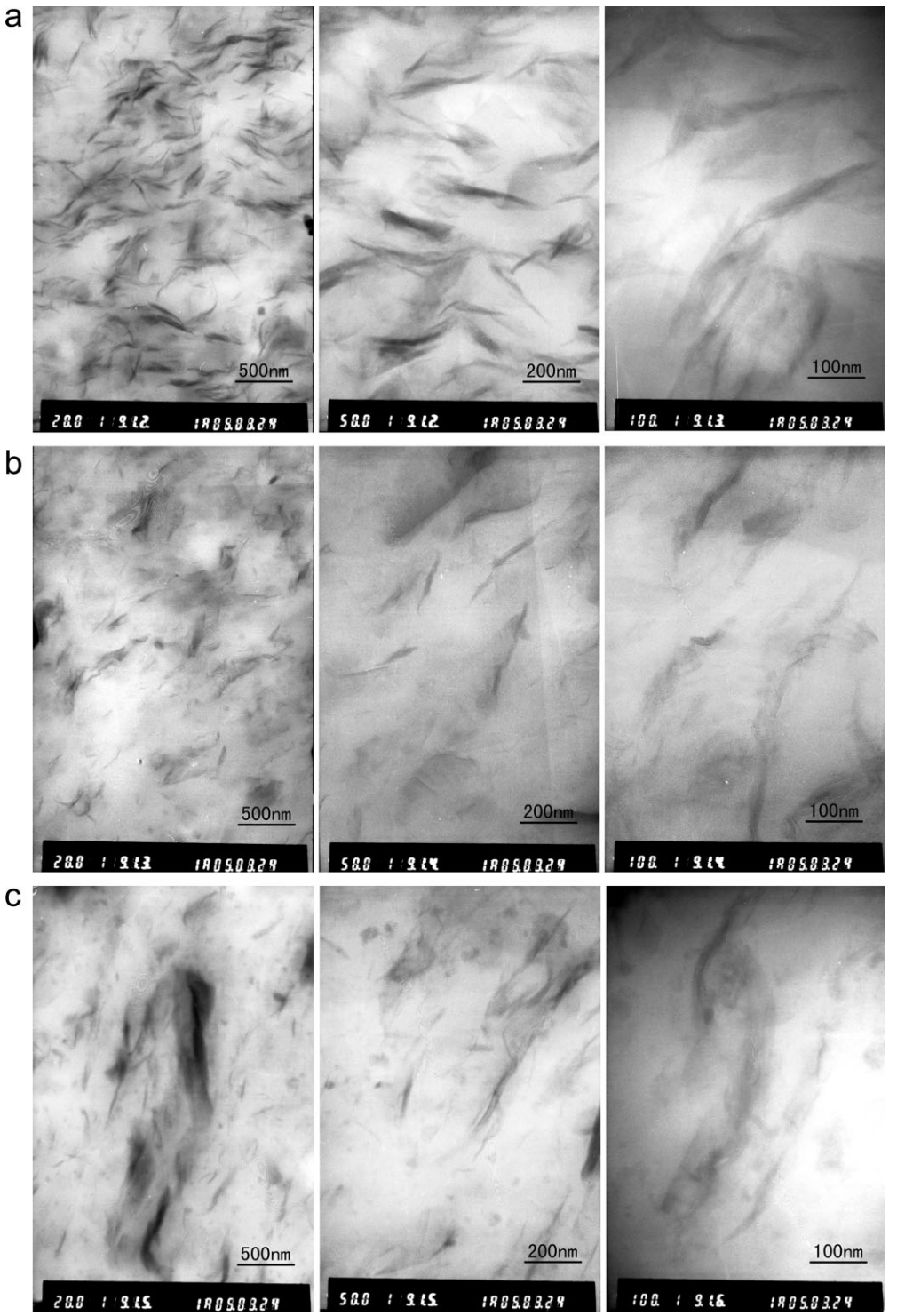

Figure 3 TEM images of NBR/OC (10 phr) nanocomposites: (a) 42NBR/OCNs, (b) 35NBR/OCNs, and (c) 26NBR/OCNs.

35NBR, and 26NBR, respectively, over the gum rubber. The improvement in the tensile strength was due to the intercalation or exfoliation of the clay in the rubber matrix, which allowed the fillers to interact more intensely with the polymer because of the higher surface area. It may also have been due to hydrogen-bond formation, as mentioned earlier. The increase was minimal in the 26NBR system because of the lowest CN content, which imparted the lowest amount of hydrogen bonding. However, the 35NBR/OCNs showed a 332% improvement over the gum. This may have been due to the larger number of hydrogen bonds formed, as the XRD results showed intercalation. The 42NBR system had the greatest

TABLE III
Mechanical Properties of the Pure NBR and NBR/OCNs (100/10)

Sample	Shore A hardness	Stress at 100%/300% (MPa)	Tensile strength (MPa)	Elongation at break (%)	Permanent set (%)	Tear strength (kN/m)
Pure 42NBR	60	1.1/1.8	3.4	470	4	19.2
42NBR/OCNs	68	1.9/4.8	16.9	543	20	30.2
Pure 35NBR	55	1.0/1.5	2.5	516	8	19.4
35NBR/OCNs	63	1.5/3.0	10.8	601	16	27.5
Pure 26NBR	55	0.9/1.2	2.0	821	8	13.7
26NBR/OCNs	60	1.4/2.2	3.7	634	12	19.1

chance of hydrogen bonding because of its highest CN content and intercalation; as shown by the XRD results, the improvement was 397% here.

The tear strength of the modified clay filled samples showed a similar trend for the NBR/OCNs. For example, the tear strength of pure 42NBR was 19.2kN/m; the tear strength increased to 30.2kN/m for the 42NBR/OCNs. The tear strength values of the gum and nanocomposites prepared by modified clay with 35NBR (26NBR) were 19.4 kN/m (13.7 kN/m) and 27.5 kN/m (19.1 kN/m), respectively. Namely, the tear strengths of the 42NBR/OCNs, 35NBR/OCNs, and 26NBR/OCNs were about 1.57, 1.42, and 1.39 times higher than that of the neat corresponding NBR. The combined action of filler dispersion and optimum interphase gave the best tear resistance among the nanocomposites tested.

The stiffness upgrade was attributed to the fact that the nanodispersed clay with the high aspect ratio possessed a higher stress-bearing capability and efficiency, and stronger interaction between the OC layers and rubber molecules because of a larger contact surface; this resulted in a more effective constraining of the motion of rubber chains, which intercalated in clay layers.

The modulus or stress of filler-filled rubber is generally dependent on many factors: filler size, filler loading, filler dispersion, interfacial interaction between the filler and matrix, and so on.[33] In general, when the interfacial interaction between the filler and rubber matrix is chemical linking, the modulus or stress at certain strains will be dramatically improved.[34,35]

There were 167, 100, and 83% and 73, 50, and 56% improvements in the stress at 100 and 300% of the 42NBR/OCNs, 35NBR/OCNs, and 26NBR/OCNs, respectively, over the pure rubber. The sharp improvement in the modulus of the 42NBR/OCNs obtained by melt intercalation implies that the interfacial interaction between the OC and rubber matrix was a strong interaction as expected; accordingly, this improvement decreased in the 35NBR/OCNs and 26NBR/OCNs.

When NBRs with different CN contents were compared, the improvement in the mechanical properties was found to be higher for NBR with a higher CN content. A less intercalated structure would impair the reinforcement effect of OC in the rubber matrix, such as in 26NBR. The results were explained with the help of XRD data, which showed that the extent of intercalation was also a function of the polarity of the rubber. The highest value of intercalation was observed for the 42NBR/OCNs. The TEM results also confirmed the XRD results. The improvement in the strength was the highest for the 42NBR/OCNs.

Gas barrier properties of the NBR/OCNs

Figure 4 highlights the barrier improvements in the NBR-based nanocomposites against nitrogen.

Compared with pure NBR, the relative nitrogen permeability of the NBR/OCNs decreased markedly by 11.5% [from 6.1×10^{-17} to 5.4×10^{-17} m^2 $(Pa\ S)^{-1}$] for the 42NBR/OCNs, by 10.4% [from 12.5×10^{-17} to 11.2×10^{-17} m^2 $(Pa\ S)^{-1}$] for the 35NBR/OCNs, and by 9.0% [from 31.1×10^{-17} to 27.3×10^{-17} m^2 $(Pa\ S)^{-1}$] for the 26NBR/OCNs, respectively, when the loading of modified clay was 10 weight parts per 100 weight parts rubber (phr). This indicates that the intercalated NBR/OCNs improved the gas barrier properties dramatically. This was attributable to the tortuosity of the penetration path because of the impermeable clay layers and stacks, and the intercalated clay layer bundles strongly restricted the motion of polymer chains, which

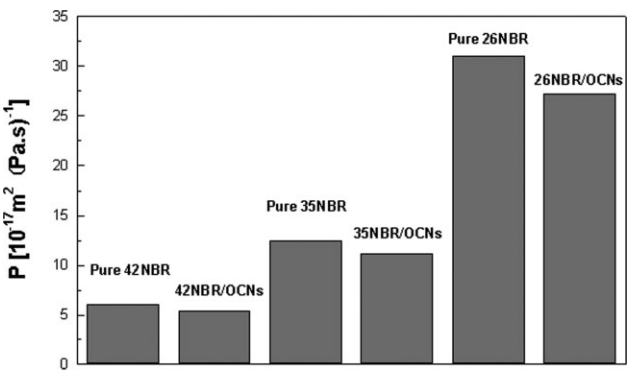

Figure 4 Nitrogen permeability (P) of pure NBR and NBR/OCNs containing 10 phr OC.

probably reduced the coefficient of the diffusion of the gas molecules. Interphase strengthening by hydrogen bonding between OH and CN groups produced even higher basal spacing for the NBR/OCNs. This characteristic was reflected in the mechanical performances (i.e., tensile strength and tear resistance) and in the reduced nitrogen permeability.

Because a more uniformly dispersed structure in the rubber matrix was the primary factor determining the gas barrier properties of the nanocomposites, the higher CN content the NBR had, the more easily the OC approached to the nanoscale, and the higher gas barrier properties were that could be easily obtained. Therefore, the permeability was controlled by the microstructure of the nanocomposites and the interaction between NBR and OC.

CONCLUSIONS

By a melt-blending process, we produced NBR/OCNs with intercalated structures and among which three grades of NBR with different CN contents (26, 35, and 42%) were studied. The NBR/OCNs were characterized by TEM and XRD. As a result, the nature of the rubber controlled the extent of intercalation and the dispersion level of the nanofiller. When all of the U-NBR/OCNs (NBR/OCNs) were compared, we discovered that the higher polarity the polymer claimed, the more easily intercalation formed, and the more homogeneous the dispersion state of silicate layers were obtained in the rubber matrix. Moreover, high pressure during vulcanization could extrude rubber chains out of the interlayer and decrease the gallery height. Pressure was a critical factor governing the final microstructure of the cured rubber/clay nanocomposites. The mechanical properties and gas barrier properties were studied for all of the compositions. When NBRs with different CN contents were compared, the improvement in the mechanical properties was found to be higher for NBRs with higher CN contents. There were 397, 332, and 85% improvements in the tensile strengths of the 42NBR/OCNs, 35NBR/OCNs, and 26NBR/OCNs, respectively, over the gum rubber. The tear strength of the samples showed a similar trend. The modulus at certain strains was dramatically improved with the increasing polarity of NBR. The permeability was controlled by the microstructure of the nanocomposites and the interaction between the NBR and OC. Compared with the pure NBR, the relative nitrogen permeability of the NBR/OCNs was reduced markedly by 11.5, 10.4, and 9.0% for the 42NBR, 35NBR, and 26NBR hybrids, respectively, when the loading of OC was 10 phr. We accepted that the polymer/clay nanocomposites having higher dispersion extents of silicate layers possessed better performances. Therefore, we can put forward some advice for obtaining desired properties in the case of NBR/clay nanocomposites prepared by melt compounding, for example, by improving the polarity of rubber in a study range.

References

1. Alexandre, M.; Dubios, P. Mater Sci Eng 2000, 28, 1.
2. Pinnavaia, T. J.; Beall, G. W. Polymer–Clay Nanocomposites; Wiley: New York, 2000.
3. Ray, S. S.; Okamoto, M. Prog Polym Sci 2003, 28, 1539.
4. Pluta, M.; Galeski, A.; Alexandre, M. J Appl Polym Sci 2002, 86, 1497.
5. Uksuki, A.; Tukigase, M. Polymer 2002, 43, 2185.
6. Giannelis, E. P. Appl Organomet Chem 1998, 12, 675.
7. Morgan, A. B.; Jeffrey, W. G. J Appl Polym Sci 2003, 87, 1329.
8. Karger-Kocsis, J.; Wu, C. M. Polym Eng Sci 2004, 44, 1083.
9. Jeon, H. S.; Rameshwaram, J. K.; Kim, G.; Weinkauf, D. H. Polymer 2003, 44, 5749.
10. Joly, S.; Garnaud, G.; Ollitrault, R.; Bokobza, L.; Mark, J. E. Chem Mater 2002, 14, 4202.
11. Mishra, J. K.; Kim, I.; Ha, C. S. Macromol Rapid Commun 2003, 24, 671.
12. Kim, J. T.; Lee, D. Y.; Oh, T. S.; Lee, D. H. J Appl Polym Sci 2003, 89, 2636.
13. Teh, P. L.; Ishak, A. M.; Hashim, A. S.; Karger-Kocsis, J.; Ishiaku, U. S. J Appl Polym Sci 2004, 94, 2438.
14. Liang, Y. R.; Wang, Y. Q.; Wu, Y. P.; Lu, Y. L.; Zhang, H. F.; Zhang, L. Q. Polym Test 2005, 24, 12.
15. Wu, Y. P.; Ma, Y.; Wang, Y. Q.; Zhang, L. Q. Macromol Mater Eng 2004, 289, 890.
16. Zhang, L. Q.; Wang, Y. Z.; Wang, Y. Q.; Sui, Y.; Yu, D. S. J Appl Polym Sci 2000, 78, 1873.
17. Wang, Y. Z.; Zhang, L. Q.; Tang, C.; Yu, D. S. J Appl Polym Sci 2000, 78, 1879.
18. Varghese, S.; Karger-Kocsis, J. Polymer 2003, 44, 4921.
19. Ma, J.; Xiang, P.; Mai, Y. W.; Zhang, L. Q. Macromol Rapid Commun 2004, 25, 1692.
20. Wang, Y. Q.; Wu, Y. P.; Zhang, H. F.; Zhang, L. Q.; Wang, B.; Wang, Z. F. Macromol Rapid Commun 2004, 25, 1973.
21. Kim, J. T.; Oh, T. S.; Lee, D. H. Polym Int 2003, 52, 1203.
22. Kim, J. T.; Oh, T. S.; Lee, D. H. Polym Int 2003, 52, 1058.
23. Zhang, H.; Zhang, Y.; Peng, Z. L.; Zhang, Y. X. Polym Test 2004, 23, 217.
24. Gatos, K. G.; Sawanis, N. S.; Apostolov, A. A.; Thomann, R.; Karger-Kocsis, J. Macromol Mater Eng 2004, 289, 1079.
25. Schön, F.; Thomanm, R.; Gronski, W. Macromol Symp 2002, 189, 105.
26. Gatos, K. G.; Thomann, R.; Karger-Kocsis, J. Polym Int 2004, 53, 1191.
27. Zhang, H.; Zhang, Y.; Peng, Z. L.; Zhang, Y. X. J Appl Polym Sci 2004, 92, 638.
28. Vaia, R. A.; Jandt, K. D.; Kramer, E. J.; Giannelis, E. P. Macromolecules 1995, 28, 8080.
29. Ray, S. S.; Okamoto, K.; Okamoto, M. Macromolecules 2003, 36, 2355.
30. Choi, D. C.; Kader, M. A.; Cho, B. H.; Huh, Y. I.; Nah, C. W. J Appl Polym Sci 2005, 98, 1688.
31. Liang, Y. R.; Lu, Y. L.; Wu, Y. P.; Ma, Y.; Zhang, L. Q. Macromol Rapid Commun 2005, 26, 926.
32. Sadhu, S.; Bhowmick, A. K. J Polym Sci Part B: Polym Phys 2004, 42, 1573.
33. Hamed, G. R. Rubber Chem Technol 2000, 73, 524.
34. Mathew, G.; Huh, M. Y.; Rhee, J. M.; Lee, M. H.; Nah, C. Polym Adv Technol 2004, 15, 400.
35. Alberola, N. D.; Benzarti, K.; Bas, C.; Bomal, Y. Polym Compos 2001, 22, 312.